EDGE DETECTION ON EDDY CURRENT IMAGE TO INCREASE DEFECT CHARACTERIZATION

B. Benoist, P. Attaoui, R. La
Commissariat à l'Energie Atomique (CEA)
Centre d'Etudes et de REcherches sur les Matériaux (CEREM)
Service des Techniques Avancées (STA)
CE Saclay, 91191 Gif-sur-Yvette Cedex, FRANCE

R. Lengellé, P. Gaillard
Université de Technologie de Compiègne (UTC)
URA 817, Compiègne, FRANCE

J. Reuchet
Commissariat à l'Energie Atomique (CEA)
Institut de Protection et de Sûreté Nucléaire (IPSN)
Département d'Etudes de Sûreté (DES)
CE Fontenay-aux-roses, 92265 Fontenay-aux-roses Cedex, FRANCE

INTRODUCTION

As the nuclear yard ages, the control of steam generator tubes (SGT) must deal with new problems. In fact new defects appear, especially in the area of the tube sheet, of the tube support or at the U-bend area. Eddy current testing using Rotating Probe Coil (absolute mode) gives a better resolution. These measurements allow smaller defects to be detected along different orientations, especially defects along the circumference in the rolling transition. Signals collected during the exploration of the tube internal wall with this coil contain the useful information which is represented in the form of a cartography (or image) for each of the signal complex components.

For example, defect characterization in kiss rolling zone (i.e. primary wall Stress corrosion cracking) consists of assessing its orientation, size and depth. Among safety regulations for SGT inspection, circumferential defect or longitudinal defect (free length above the tube sheet is less than 13 mm) result in the plugging of the tube.

Expertise of SG of 900 MW PWR's using eddy current multifrequency (F1=500 kHz, F2=240 kHz, F3=100 kHz and F4=30 kHz) testing using Rotating Probe Coil (RPC) consists of scanning the inner surface with an absolute coil (diameter equal to 1 mm). The scanning is helical (the step is 0.5 mm, figure 1). The expertise consisted of examining the images of each component (X or Y) and of each frequency response (F1, F2, F3 and F4).

The paper deals with the automatic characterization of defects through the application of image processing tools. The aim is to produce a planar representation of the

Review of Progress in Quantitative Nondestructive Evaluation, Vol. 15
Edited by D.O. Thompson and D.E. Chimenti, Plenum Press, New York, 1996

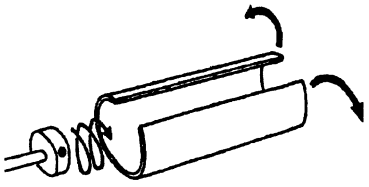

Figure 1. Path described by the rotating probe during data acquisition.

defect architecture in order to ascertain its size and orientation. The techniques used are based on application of a skeletonization algorithm which requires that images are available in binary form. The procedure is automatic : edge detection is used to determine the threshold before skeletonizing. This technique is thoroughly described.

DEFECT IDENTIFICATION USING IMAGE PROCESSING

The purpose of identifying defects is to provide the primary orientation and associated size of a defect. The idea behind this analysis was to provide a "skeleton", or planar filiform representation, of the defect architecture. This representation would allow direct measurement of the dimensions of such defects and provide an immediate visual indication of the direction of a defect which semi-relief mapping does not allow owing to its subjective nature (three-dimensional representations being especially subject to shadowing and to the viewing angle).

Given this, grid and frame maps need to be replaced by pixel mapping, whereby the grey scale corresponds to the amplitude values of an eddy current signal component, as measured at each grid point on the tube. To apply image processing algorithms, raw data must be quantized into an image of 256 gray levels . Hence, skeletonizing the gray levels image will result binary image where : level 1 represents defect region and level 0 represents background region.

THRESHOLDING USING CONTOUR DETECTION

The procedure for obtaining a satisfactory binary image which correctly takes into account the shape of the defect is somewhat intricate, especially given that the aim is to produce a wholly automated procedure.

Standard thresholding methods based on observations of raw histogram representations of images, do not yield good results. Histogram manipulation techniques, such as levelling and stretching, have not made any noticeable improvements; however, stretching significantly enhances image contrast and will therefore be applied here.

Thresholding may be associated with contour detection in the sense that, in both cases, the aim is to isolate an object from its environment. In fact, the contours generally correspond to sudden changes in the physical or geometrical properties of objects within a given view, or more exactly in this application, to changes caused by defects in the material. The idea is therefore to detect the defect contours, with a high degree of precision, in order to compute a mean value for the grey scales associated with the pixels

selected. This value gives a good approximation of the threshold to be applied in order to ascertain the correct binary shape of the defect.

The contour detection algorithm chosen for this work is based on the Laplacian zero-crossings property [2]. This concept was initially based on convolving an image with the Laplacian of a 2-D Gaussian function. As derived method, Shen and Castan proposed an optimal filter for edge detection : the Difference Recursive Filter (DFR) [4]. The Recursive Filter with two coefficients is defined as :

$$f(u) = a_0 \times a_1^{|u|} \qquad (1).$$

The Laplacian convolved with the image can be calculated by the difference between the input x(u) and output y(u) of this filter [5] :

$$y(u) - x(u) \propto \nabla^2 f * x(u) \qquad (2)$$

where * means convolution.

This method was proved less sensitive to noise and sharper for edge detection. Comparaison between the gaussian filter and DRF is thoroughly described by Shen and Castan [5]. DRF algorithm not only allows good contour detection within images, but also offers length and amplitude selection criteria in relation to the segments which are to be retained. DRF was chosen for edge detection on eddy current image. In order to adapt this method to eddy current images, additional models needed to be developed to differentiate between segment defect contours and image artefacts. Application of a convolution integral could yield differing results depending on the image trajectory. In the case of contour detection, the method could be used to favour given directions, thus providing a means of eliminating noise contours (not defect contour). This method is used below. The DRF method is applied to maps by tracing the points in the two directions available, namely line by line and column by column. The resultant images differ mainly with regard to the detected noise contours, which are not necessarily identical, while the defect contours remain very similar.

This asymmetrical detection method may then be used to multiply out the two binary images of the contours. This AND logic then provides an image in which only the contours common to both axes remain, in other words, those relating to the defect. Those artefacts which remain after the above-detailed processing is finished, may then be differentiated from others by their variance. The variance image is made up of all the contour points which have as their new value, the result from calculating out the variance in the window in question. The values for artefacts resulting from this method are much lower than for those values for a defect, and can be seen to resemble that of the adaptive gradient used in the DRF method.

By applying thresholding to this variance image, another selection method can be obtained. However, the segments shall be considered here as entities, thus no longer needing work on a point-by-point basis. Each segment is defined by its maximum value and the thresholding test is carried out with respect to this value in order to decide whether or not to retain the segment in question. Indeed, point-by-point thresholding can lead to the elimination of significant contour points whereas "segment thresholding" avoids this problem. The threshold value is estimated heuristically to equal: mean - ¼ standard deviation (calculated using the maximum points for each segment).

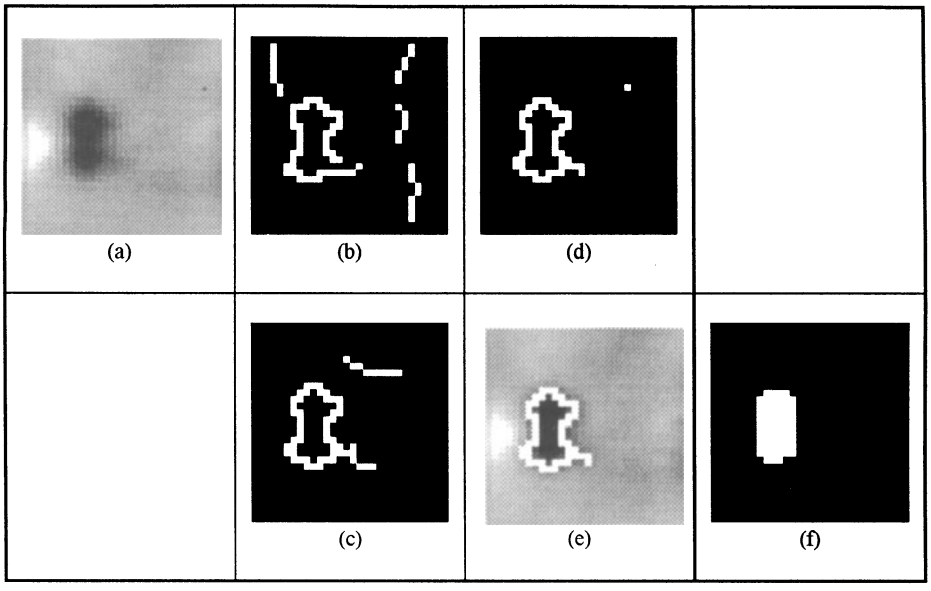

Figure 2. The contour processing sequence

Highly satisfactory results are obtained owing to all the artefacts being eliminated in the vast majority of the images. This set of image processing modules forms an automatic sequence allowing the processing of any image type without the need for any parameter adjustment. Below (figure 2) is one example of how the various processing modules may be applied:

(a): grey-scale image of the defect,
(b) and (c): contour detection along two axes,
(d): result from using AND logic on (b) and (c),
(e): contour selection after thresholding on the variance, then superimposed on image (a),
(f): binary image following thresholding.

The contours thus selected will then allow a threshold value corresponding to the mean grey-scale value of the pixels selected as contour points, to be computed. The result from the thresholding is shown as (f) in the following Figure 2.

DEFECT SIZE DETERMINATION

Once a coherent image of the defect is obtained, the skeleton algorithm may then be applied. Several analogies may be used to outline the concept of skeletonizing, the one most often used being that of the spreading of a bush fire. Imagine if a fire was made to spread from the boundaries of the object to be skeletonised, the fire would spread at a constant speed towards the centre of the object, and eventually die out once there was nothing left to burn, leaving behind lines where the fire stopped. These lines represent the skeleton of the object. A more mathematical representation may also be used, this time using sets and specifically the notion of the skeleton of a set E in a Euclidian space [6].

The skeleton of a set E is defined as the joining of the centres of the largest discs which can be contained in the set E.

For each point x which belongs to E, let D(x) be the largest disc, having centre x, such that D(x) is a sub-set of E. Thus x belongs to skeleton S if another disc D' is not

present, the centre of which may differ from x, and such that D' contains D(w) and is included in E.

Figure 3 shows how a skeleton is constructed in the case of an isosceles triangle (-a-). Point x is part of the skeleton as there are no other discs included in the triangle containing D(x) (-b-). Point w does not belong to the skeleton as D(w) is encompassed by D' which is itself included in the triangle (-c-).

If one takes the previous example, calculating the skeleton gives the result shown in Figure 4, superimposed over the grey-scale image. The defect is a small longitudinal crack of length estimated at 4 mm.

All of the tests carried out on a library of known defects have supplied size measurements to within ± 25% (i.e. within the specifications laid down by safety authorities) while orientation has always been determined correctly. The accuracy of defect characterization is obviously directly related to the quality of the physical measurements.

As an example of the mapping technique, consider first of all data collected from a steam generator tube removed from Dampierre Nuclear Power Plant. The tube has an expansion region where several small longitudinal cracks have appeared. However, size comparisons cannot be made in this instance as a non-destructive analysis method was used.

Figure 5 shows a grey-scale image where each defect has been individually processed in order to detect the contours; Figure 6 shows the results obtained from skeletonization, and reveals cracks with an estimated length of between 1.5 and 2.5 mm.

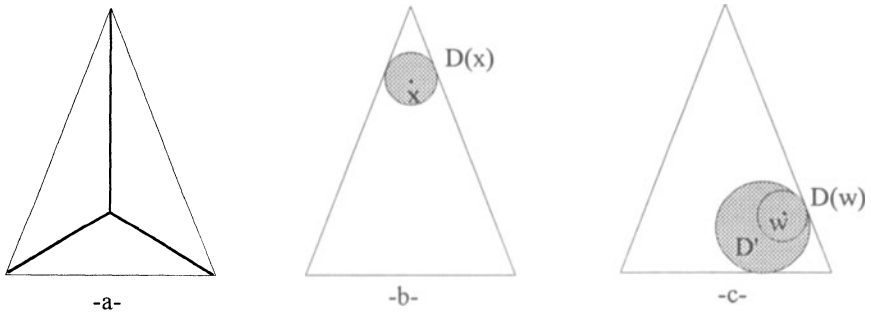

Figure 3. Construction of a skeleton

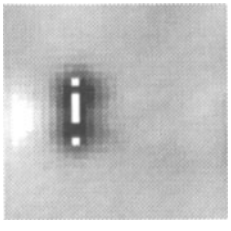

Figure 4. Skeleton superimposed over the original image

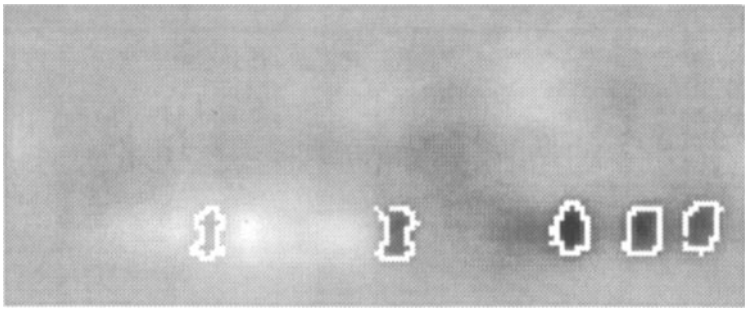

Figure 5. The contours of each separately determined defect superimposed over the original image.

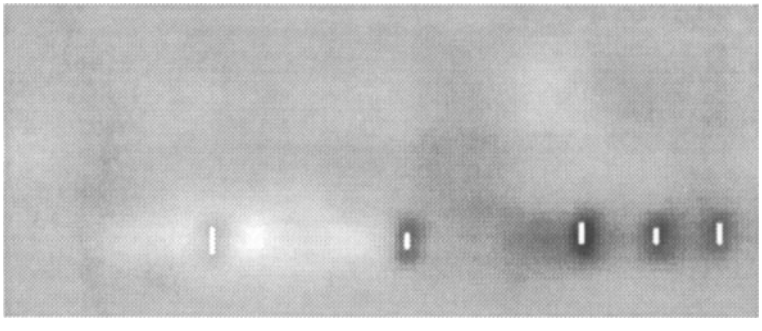

Figure 6. Skeletonization results for each individual defect

A further example of defect characterization is given by a tube subjected to thermal and chemical treatment to simulate steam generator conditions, but over a much shorter timescale to accelerate ageing. The tube was finally destructively analysed to determine the resultant defects. The tube had developed a series of longitudinal hairline cracks and two adjacent groups of mosaic-patterned hairline cracks oriented more or less obliquely. The defects originated on the outer surface of the tubes. Figure 7 shows the results from the destructive analysis, while Figure 8 shows a map of one of the components, and finally, Figure 9 shows a grey-scale representation where the skeleton has been superimposed and the crack dimensions estimated.

The map of component F1y (where F1 is the inspection frequency, 500 kHz, and y the signal projection) clearly shows the three crack networks, including the two adjacent groups, while the characterization correctly gives both the sizes and the main orientation of the three defect groups.

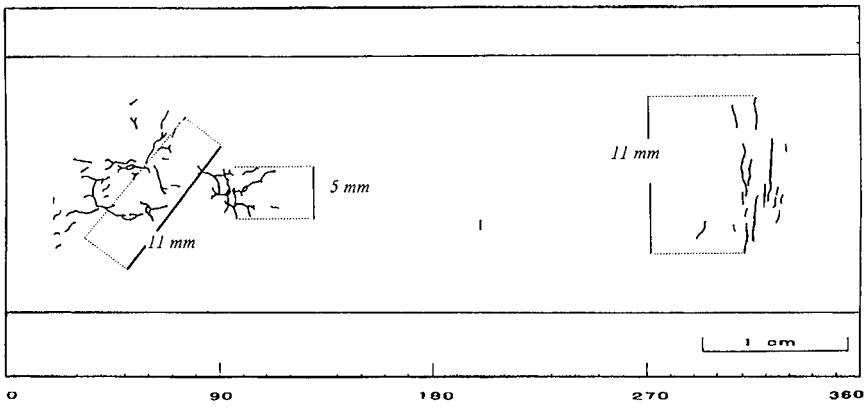

Figure 7. Results from the destructive analysis of the tube.

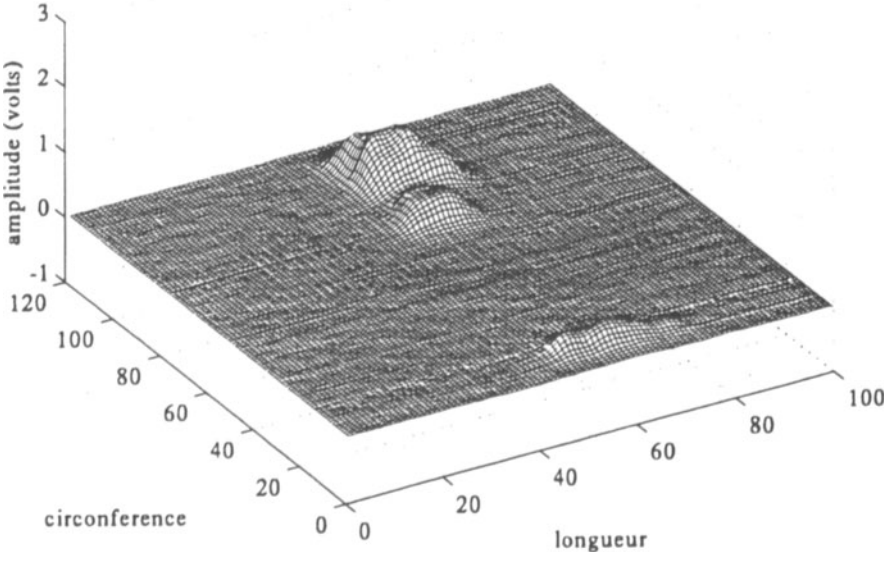

Figure 8. Map of the F1y component

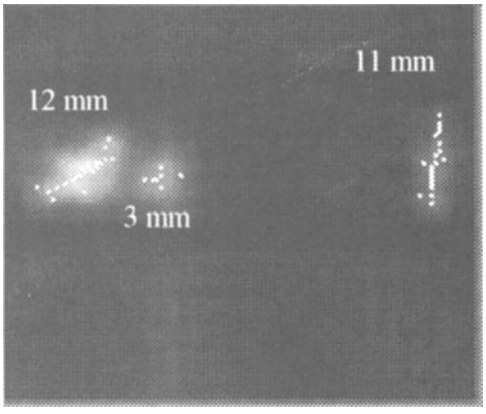

Figure 9. Skeletonization results

CONCLUSION

We have adapted tools for the processing and analysis of eddy current maps obtained from the inspection of steam generator tubes using an absolute coil probe. This includes the selection and enhancement of image processing tools best suited to defect characterization. The aim of this characterization was to ascertain the predominant size and orientation of the defects detected. A skeleton type representation was used which takes account of defect architecture. The skeletonization techniques were applied to the binary images, although obtaining these gave rise to a number of difficulties. Simple thresholding using histograms, for instance, is considered too crude to be used. Instead, contour detection techniques were adopted to calculate a threshold value using the mean grey-scale value of the pixels selected as contour points. The contour detection algorithm used included a number of parameters which were successfully set and adapted to the eddy current images (with the aim of obtaining an automated processing sequence). In addition, this algorithm has been enhanced and developed further using new modules. The results for single defects are highly satisfactory as the associated error is around ± 25% for size measurements, while the orientation is almost always correctly determined. These estimates are of course related to the accuracy of the physical measurement technique. This work has been carried out in accordance with the requirements laid down by the safety authorities on the improvement of defect characterization effectiveness and accuracy.

REFERENCES

1. B. DAVID, M. PIGEON, C. BIRAC, Application de l'outil informatique aux mesures effectuées par courants de Foucault : conception, réalisation et utilisation de cartographies CF, 7th International Conference on NDT, Grenoble, janvier 85.
2. Rafael C. GONZALEZ, Richard E. WOODS, Digital Image Processing Addison-Wesley publishing company 1992.
3. D. MARR, E. HILDRETH, Theory of edge detection proceedings of the royal society of London, Vol B207, 1980, pp 187-217
4. Jun SHEN, Serge CASTAN, A new algorithm for edge detection, 5th conference on Pattern Recognition and Artificial Intelligence, Grenoble, 1985, pp 201-213.
5. Jun SHEN, Serge CASTAN, An optimal linear operator for edge detection, Proc. Computer Vision and Pattern Recognition, Miami, 1986, pp 109-114.
6. C.R. GIARDINA, E.R. DOUGHERTY, Morphological methods in image and signal processing, Prentice Hall, 1988.